

# DROOP-CONTROLLED INVERTERS ARE KURAMOTO OSCILLATORS

JOHN W. SIMPSON-PORCO, FLORIAN DÖRFLER & FRANCESCO BULLO\*

**Abstract.** Motivated by the recent interest in smart grid technology and by the push towards distributed and renewable energy, we study the parallel operation of DC/AC inverters in a lossless microgrid. We show that the parallel interconnection of DC/AC inverters equipped with conventional droop controllers is precisely described by the Kuramoto model of coupled phase oscillators. This novel description, together with results from the theory of coupled oscillators, allows us to characterize the behavior of the network of inverters. Specifically, we provide a necessary and sufficient condition for the existence of a synchronized solution that is unique and locally exponentially stable. Remarkably, we find that the existence of such a synchronized solution does not depend on the selection of droop coefficients. We prove without additional assumptions that the inverters share the network power demand in proportion to their power ratings if and only if the droop coefficients are selected proportionally, and we characterize the set of feasible loads which can be serviced. Moreover, we make precise and quantitative the idea of regulating the frequency of the system to a nominal value via an outer secondary control loop. We propose a secondary controller which dynamically regulates the system frequency in the presence of a time-varying load. Our results hold without assumptions on identical line characteristics or voltage magnitudes.

**Key words.** inverters; power-system control, smart power applications, synchronization, coupled oscillators, Kuramoto model, distributed control

**1. Introduction.** Microgrids appear to be the most natural extension of classical energy generation to a renewable and distributed setting. A *microgrid* is a low-voltage electrical network, heterogeneously composed of distributed generation, storage, load, and managed autonomously from the larger primary network. Microgrids are able to connect to the wide area electric power system (WAEPS) through a Point of Common Coupling (PCC), but are also able to “island” themselves and operate independently. Energy generation within a microgrid can be highly heterogeneous, combining photovoltaic farms, wind turbines, thermo-solar power, biomass, geothermal, and gas micro-turbines. Many of these devices generate either variable frequency AC power or DC power, and are therefore interfaced with a synchronous AC microgrid via power electronic devices called DC/AC *power converters*, or simply *inverters*. In islanded operation, inverters are operated as *voltage sourced inverters* (VSIs), which act much like ideal voltage sources. It is through these VSIs that actions must be taken to ensure synchronization, security, power balance and load sharing in the network.

**Literature Review.** A primary topic of interest within the microgrid community is the problem of accurately sharing both active and reactive power among a bank of inverters operated *in parallel*. Such a network is depicted in Figure 1.1, in which each inverter transmits power directly to the load. As detailed in the recent review [1], power sharing techniques generally fall into three categories, namely master/slave, current sharing, and “droop” methods. The first two methods unfortunately require some form of on-line global communication among the units, and introduce

---

\*Center for Control, Dynamical Systems, and Computation, University of California, Santa Barbara, Santa Barbara, CA 93106, USA, (e-mail: [johnwsimpsonporco,dorfler,bullo]@engineering.ucsb.edu). This work was supported in part by the National Science Foundation NSF CNS-1135819 and by the National Science and Engineering Research Council of Canada.

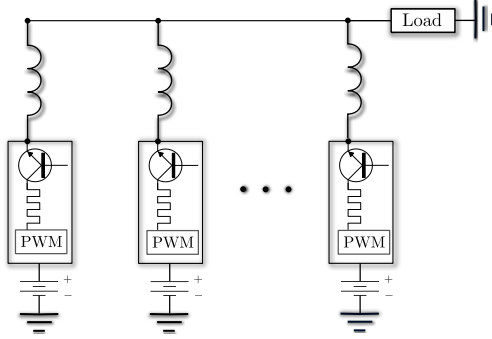


FIG. 1.1. Schematic of inverters operating in parallel in a microgrid. The horizontal line is aesthetic, and represents a single electrical node. The inverters convert the externally supplied DC power to AC power in order to satisfy the power demand at the load.

a common failure point for the entire system. This lack of redundancy and need for communication makes these techniques undesirable in a truly distributed “plug and play” setting.

The droop controllers however do not require explicit communication between inverter units during operation. The original reference for this methodology appears to be [2], where Chandorkar *et. al.* introduce what we will refer to as the *conventional droop controller*. The conventional droop controller is a heuristic based on physical intuition gleaned from the study of high-voltage WAEPS, and at its core relies on the decoupling of active and reactive power for small power angles and non-mixed line conditions. It is well known that for lossless lines and small power angles, active power flows are controlled by the power angles while reactive power flows are controlled by the differences in bus voltages. In this case, the droop method attempts to emulate the behavior of a classical synchronous generator by imposing an inverse relation at each inverter between frequency and active power injection, and between the bus voltage and reactive power injection [3]. Under other network conditions, the method takes different forms [4, 5]. Some representative references for the basic methodology are [6, 7, 8, 9, 10] and [11]. Small-signal stability analyses are presented under various assumptions in [12, 13, 14, 15, 16] and the references therein. The recent work [17] highlights many of the drawbacks of the conventional droop method.

Alternative distributed controllers have also been proposed. In [18], a control scheme is presented in which the each inverter is designed to emulate the classic swing equations, and in this sense *truly* behave as a synchronous generator. This scheme requires the presence of an additional energy source to mimic the kinetic energy stored in the rotating mass of a generator. Since a microgrid is naturally distributed and heterogeneous in nature, it is an ideal application area for tools developed in distributed control and multi-agent systems, see [19, 20, 21]. A synchronization approach was put forward in [22] in which inverters are modeled as passive oscillators. A distributed scheme for reactive power compensation in a grid-connected microgrids is presented in [23]. A “self-organizing” strategy for grid-connected inverters is put forward in [24], in which the inverters coordinate their power injections through an asynchronous communication network.

Another set of literature relevant to our investigation is that pertaining to synchronization of coupled oscillators, in particular the classic and celebrated *Kuramoto model* introduced in [25]. A generalized variant of this model considers  $n \geq 2$  cou-

pled oscillators, each represented by a phase  $\theta_i \in \mathbb{S}^1$  (the unit circle) and a natural frequency  $\omega_i \in \mathbb{R}$ . The system of coupled oscillators obeys the dynamics

$$\dot{\theta}_i = \omega_i - \sum_{j=1}^n a_{ij} \sin(\theta_i - \theta_j), \quad i \in \{1, \dots, n\}, \quad (1.1)$$

where  $a_{ij} \geq 0$  is the coupling strength between the oscillators  $i$  and  $j$ .

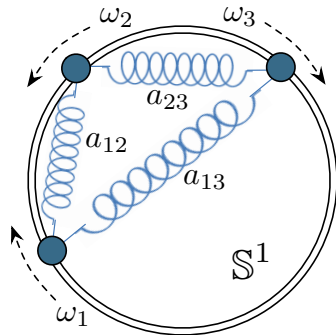


FIG. 1.2. Mechanical analog of a Kuramoto oscillator network.

A nearly perfect mechanical analog of the Kuramoto model (1.1) is shown in Figure 1.2. The Kuramoto model (1.1) can be visualized as a group of  $n$  kinematic particles constrained to rotate around the unit circle. The particles rotate with preferred directions and rotational speeds specified by the natural frequencies  $\omega_i$ , and are connected together by elastic springs of stiffness  $a_{ij}$ . In comparison to the mechanical analog in Figure 1.2, the Kuramoto oscillators (1.1) are inertialess and do not collide with one another. The rich dynamic behaviour of the system (1.1) arises from the competition between the tendency of each oscillator to align with its natural frequency  $\omega_i$ , and the synchronization enforcing coupling  $a_{ij} \sin(\theta_i - \theta_j)$  with its neighbors. The literature on Kuramoto oscillators is vast, and the model has attracted tremendous interest from the physics, control, dynamical systems, and neuroscience communities. We refer to the recent surveys [26, 27, 28, 29, 30, 31, 32] for various applications and theoretic results.

**Review of Frequency-Droop Method.** The *frequency-droop method* is the foundational technique for inverter control to ensure that the *active power* demand at the load is shared among a bank of parallel VSIs in proportion to their power ratings. In case of inductive output impedance, the controller specifies an instantaneous change in the frequency  $\omega_i$  of the voltage signal at the  $i^{\text{th}}$  inverter according to

$$\omega_i = \omega^* - n_i(P_{e,i} - P_i^*), \quad i \in \{1, \dots, n\}, \quad (1.2)$$

where  $\omega^*$  is a rated frequency,  $P_{e,i}$  is the active electrical power injection at bus  $i$ , and  $P_i^*$  is the nominal active power injection when operated at the rated frequency. The parameter  $n_i > 0$  is referred to as the *droop coefficient*. It is clear from (1.2) that for  $P_i \neq P_i^*$ , the operating frequency of the  $i^{\text{th}}$  inverter deviates from its nominal rated frequency.

**Limitations of the Literature.** Despite forming the foundation for the operation of paralleled VSIs, the droop control law (1.2) has never been subject to a full

nonlinear analysis [17]. To the authors’ knowledge, no conditions have ever been presented under which the closed-loop system (1.2) possess a synchronous steady state, nor have any statements been made about the convergence rate to such a steady state should one exist. Stability results that are presented rely on analysis of a linearized model, and sometimes come packaged with assumptions involving certain admittances in the system being small compared to others. Stability and power sharing results are typically presented for the case of two inverters, with the corresponding generalized calculation to larger networks left implicit or unclear. No analytical guarantees are given in terms of performance.

**Contributions.** The contributions of this paper are as follows. We begin with our key observation that the nonlinear differential equations governing the closed-loop system of a microgrid under the frequency-droop controller can be equivalently rewritten as a non-uniform multi-rate Kuramoto model of first-order phase-coupled oscillators. This insight allows us to give several interesting interpretations of the resulting feedback interconnection. We present a necessary and sufficient condition for the existence of a stabilized solution of the closed-loop, and provide an explicit bound on the local convergence time scale. In particular, we show that the method is stabilizing independent of the droop coefficient values, and that the steady state solution is unique and locally exponentially stable. In comparison to the existing literature, we show that if the droop coefficients are selected in proportion to the rated power values, the inverters share power proportionally without assumptions on large output impedances or identical voltage magnitudes. We then examine in detail the idea of using a “secondary” control loop to regulate the system frequency to a nominal value. We propose a secondary controller and show that it is locally stabilizing, without relying on any additional assumptions such as a time scale separation between the primary and secondary control loop.

**Paper Organization.** The remainder of this section introduces some notation and reviews some fundamental material from algebraic graph theory, power systems and coupled oscillator theory. In Section 2 we motivate the mathematical models used throughout the rest of the work, discussing both inverter and network modeling. In Section 3 we perform a full nonlinear stability analysis of the conventional frequency-droop method, and present the results described in the contributions section above. Finally, Section 4 concludes the paper presents directions for future work.

**Preliminaries and Notation.** *Sets, vectors and functions:* Given a finite set  $\mathcal{V}$ , let  $|\mathcal{V}|$  denote its cardinality. Given an  $n$ -tuple  $(x_1, \dots, x_n)$ , let  $x \in \mathbb{R}^n$  be the associated vector. For a complex valued 1D-array  $\{x_i\}_{i=1}^n$ , we let  $\text{diag}(\{x_i\}_{i=1}^n)$  be the associated diagonal matrix. We denote the  $n \times n$  identity matrix by  $I_n$ . Let  $\mathbf{1}_n$  and  $\mathbf{0}_n$  be the  $n$ -dimensional vectors of all ones and all zeros. For a vector  $x \in \mathbb{R}^n$ , we define  $\mathbf{sin}(x) \triangleq (\sin(x_1), \dots, \sin(x_n))^T \in \mathbb{R}^n$ .

*Algebraic graph theory:* A weighted graph  $G$  without self-loops is a triple  $G = (\mathcal{V}, \mathcal{E}, L)$  where  $\mathcal{V}$  is a set of nodes,  $\mathcal{E} \subseteq \mathcal{V} \times \mathcal{V}$  is a set of edges, and  $L \in \mathbb{C}^{|\mathcal{V}| \times |\mathcal{V}|}$  is the *Laplacian matrix* of the graph. If a number  $\ell \in \{1, \dots, |\mathcal{E}|\}$  and an arbitrary direction is assigned to each edge  $(i, j) \in \mathcal{E}$ , the *oriented node-edge incidence matrix*  $B \in \mathbb{R}^{|\mathcal{V}| \times |\mathcal{E}|}$  is defined component-wise as  $B_{k\ell} = 1$  if node  $k$  is the sink node of edge  $\ell$  and as  $B_{k\ell} = -1$  if node  $k$  is the source node of edge  $\ell$ , with all other elements being zero. For  $x \in \mathbb{R}^n$ ,  $B^T x$  is the vector with components  $x_i - x_j$ , with  $\{i, j\} \in \mathcal{E}$ . If  $\text{diag}(\{a_{ij}\}_{\{i,j\} \in \mathcal{E}}) \in \mathbb{C}^{n \times n}$  is the diagonal matrix of edge weights, then  $L = B \text{diag}(\{a_{ij}\}_{\{i,j\} \in \mathcal{E}}) B^T$ . Where confusion can arise, we will explicitly write  $L(a_{ij})$  to

make explicit the weights used in the calculation of the Laplacian. If the graph is connected, then  $\ker(B^T) = \ker(L) = \text{span}(\mathbf{1}_n)$ . Moreover,  $L$  is positive semidefinite, with eigenvalues  $\lambda_j(L)$ ,  $j \in \{1, \dots, |\mathcal{V}|\}$ , which can be ordered as  $0 = \lambda_1(L) < \lambda_2(L) \leq \dots \leq \lambda_{|\mathcal{V}|}(L)$ . We will briefly make use of the *Moore-Penrose inverse*  $L^\dagger$  of the Laplacian matrix  $L$ . If  $U \in \mathbb{C}^{|\mathcal{V}| \times |\mathcal{V}|}$  is an orthonormal matrix of eigenvectors of  $L$ , the singular value decomposition yields  $L = U \text{diag}(0, \lambda_1, \dots, \lambda_n) U^T$ . The pseudoinverse  $L^\dagger$  of  $L$  is then defined by  $L^\dagger \triangleq U \text{diag}(0, 1/\lambda_1, \dots, 1/\lambda_n) U^T$ , and the identity  $LL^\dagger = L^\dagger L = I_n - \frac{1}{n} \mathbf{1}_{|\mathcal{V}|} \mathbf{1}_{|\mathcal{V}|}^T$  can be shown to hold. The *effective impedance* between nodes  $i$  and  $j$  is defined by  $Z_{ij} \triangleq L_{ii}^\dagger + L_{jj}^\dagger - 2L_{ij}^\dagger$ .

*Geometry on the  $n$ -torus:* The set  $\mathbb{S}^1$  denotes the *unit circle*, an *angle* is a point  $\theta \in \mathbb{S}^1$ , and an *arc* is a connected subset of  $\mathbb{S}^1$ . With a slight abuse of notation, let  $|\theta_1 - \theta_2|$  denote the *geodesic distance* between two angles  $\theta_1, \theta_2 \in \mathbb{S}^1$ . The  $n$ -torus  $\mathbb{T}^n = \mathbb{S}^1 \times \dots \times \mathbb{S}^1$  is the Cartesian product of  $n$  unit circles. For  $\gamma \in [0, \pi/2)$  and a given graph  $G = (\mathcal{V}, \mathcal{E}, \cdot)$ , let  $\overline{\Delta}_G(\gamma) = \{\theta \in \mathbb{T}^{|\mathcal{V}|} : \max_{\{i,j\} \in \mathcal{E}} |\theta_i - \theta_j| \leq \gamma\}$  be the closed set of angle arrays  $\theta = (\theta_1, \dots, \theta_n)$  with neighboring angles  $\theta_i$  and  $\theta_j$ ,  $\{i, j\} \in \mathcal{E}$  no further than  $\gamma$  apart. We also define  $\Delta_G(\gamma)$  as the interior of  $\overline{\Delta}_G(\gamma)$ . Note that  $\overline{\Delta}_G(\gamma)$  depends on the graph  $G$  through its edge set  $\mathcal{E}$ .

*Power flow equation:* Consider a lossless, synchronous AC electrical network with  $n$  nodes, purely inductive admittance matrix  $Y \in \mathbb{C}^{n \times n}$ , nodal voltage magnitudes  $E_i > 0$ , and nodal voltage phase angles  $\theta_i \in \mathbb{S}^1$ . The active electrical power  $P_{e,i} \in \mathbb{R}$  injected into the network at node  $i$  is given by [3]

$$P_{e,i} = \sum_{j=1}^n E_i E_j |Y_{ij}| \sin(\theta_i - \theta_j), \quad i \in \{1, \dots, n\}. \quad (1.3)$$

*Synchronization:* Consider the first order phase-coupled oscillator model (1.1) defined on a graph  $G = (\mathcal{V}, \mathcal{E}, L(a_{ij}))$ . A solution  $\theta : \mathbb{R}_{\geq 0} \rightarrow \mathbb{T}^{|\mathcal{V}|}$  of (1.1) is said to be *synchronized* if (a) there exists a constant  $\omega_{\text{sync}} \in \mathbb{R}$  such that for each  $t \geq 0$ ,  $\dot{\theta}(t) = \omega_{\text{sync}} \mathbf{1}_{|\mathcal{V}|}$  and (b) there exists a  $\gamma \in [0, \pi/2)$  such that  $\theta(t) \in \overline{\Delta}_G(\gamma)$  for each  $t \geq 0$ . That is, every oscillator rotates at the constant angular speed  $\omega_{\text{sync}}$ , with all pair-wise geodesic distances *along edges* less than or equal to  $\gamma$ .

## 2. Problem Setup for Microgrid Analysis.

*Inverter Modeling:* DC/AC inverters are power electronic devices with complex nonlinear characteristics. A DC source is connected to the input of a bridge circuit consisting of insulated gate bipolar transistors (IGBTs) arranged as switches, with an externally applied pulse-width modulation (PWM) signal being used to control the voltage level at the output of the inverter bridge. The voltage level at the output may therefore only take a discrete set of values, bounded within the limits set by the original DC source, and the PWM signal is designed to approximate a desired sinusoid at the output. The output voltage is then filtered to remove switching harmonics and maintain a low level of total harmonic distortion (THD). If the PWM switching frequency is chosen much faster than the frequency of the desired output signal, the switched signal averages locally to the desired reference signal. This procedure is sometimes augmented with local control loops to stabilize the voltage and/or current output. The end result is that an inverter can be modeled to a good approximation as a controlled voltage source behind a reactance, an approximation which is standard in the microgrid literature. Further modeling explanation can be found in [33, 34, 35] and the references therein, with [36] offering a more detailed analysis of the switching electronics.

*Islanded Microgrid Modeling:* A mathematical model of a parallel microgrid is that of a weighted graph  $G = (\mathcal{V}, \mathcal{E}, Y)$ , where  $\mathcal{V} = \{v_0, \dots, v_n\}$  is the set of nodes,  $\mathcal{E}$  is the set of edges, and  $Y \in \mathbb{C}^{(n+1) \times (n+1)}$  is the bus admittance matrix of the network. We let nodes  $1, \dots, n$  correspond to the inverter connection points, and let the  $0^{\text{th}}$  node be the load point. With this, the node-edge incidence matrix of  $G$  has the simple form

$$B = [-\mathbf{1}_n \quad I_n]^T. \quad (2.1)$$

For  $i \in \{1, \dots, n\}$ ,  $\sqrt{-1} \cdot b_{i0}$  is the admittance of the edge between the inverter  $i$  and the load. The output impedance of the inverter can be controlled to be purely imaginary, and we absorb its value into the line susceptance  $b_{i0} < 0$ . The network admittance matrix  $Y$  is then given by  $Y = \sqrt{-1} \cdot B \text{diag}(\{b_{i0}\}_{i=1}^n) B^T$ . To the  $i^{\text{th}}$  node we assign a voltage signal of the form  $E_i(t) = E_i \cos(\omega_0 t + \theta_i)$ , where  $\omega_0 > 0$  is the nominal angular frequency,  $E_i > 0$  is the RMS voltage, and  $\theta_i \in \mathbb{S}^1$  is the voltage phase angle. From (1.3), the  $i^{\text{th}}$  inverter therefore injects a time-averaged real power  $P_{e,i} = E_i E_0 |Y_{i0}| \sin(\theta_i - \theta_0)$ . We will assume this value is restricted to the interval  $[0, \bar{P}_i]$  where  $\bar{P}_i \leq E_i E_0 |Y_{i0}|$  is the *rating* of inverter  $i$ .

**3. Nonlinear Analysis of Frequency Droop Control.** We now connect the frequency-droop method (1.2) to a network of first-order phase-coupled oscillators akin to (1.1). In what follows we restrict our attention to the analysis of active power flows, and assume the voltage magnitudes at each bus to be fixed, but not necessarily identical. Specifically, we consider the problem of stable operation and proportional active power sharing among  $n$  paralleled inverters in a lossless, islanded microgrid. We assume that each inverter has precise measurements of its time-averaged active power injection  $P_{e,i}$  and of its frequency  $\theta_i(t)$  — see [33] for details regarding this estimation.

An equivalent reformulation of the droop controller (1.2) at inverter  $i \in \{1, \dots, n\}$  is given by

$$D_i \dot{\theta}_i = P_i^* - P_{e,i}, \quad (3.1)$$

where  $D_i > 0$ ,  $P_i^* \in [0, \bar{P}_i]$  is a selected nominal value and  $P_{e,i}$  is the VSI's active electrical power injection<sup>†</sup>. Indeed, a quick inspection shows that (3.1) is a rewriting of (1.2) with  $\omega_i = \omega_0 + \dot{\theta}_i$ ,  $D_i = n_i^{-1}$ , and  $\omega^* = \omega_0$ . The reason for this rewriting is to make clear the connection to coupled oscillators which we will now establish. Note that  $\dot{\theta}_i$  is the *deviation* of the frequency at inverter  $i$  from the nominal frequency  $\omega_0$ . Using the active load flow equations (1.3), we obtain

$$D_i \dot{\theta}_i = P_i^* - E_i E_0 |Y_{i0}| \sin(\theta_i - \theta_0), \quad i \in \{1, \dots, n\}. \quad (3.2)$$

For a constant power load  $P_0^* < 0$  we must also satisfy the (lossless) power balance equation

$$0 = P_0^* + \sum_{i=1}^n P_{e,i} = P_0^* + \sum_{i=1}^n E_i E_0 |Y_{i0}| \sin(\theta_i - \theta_0). \quad (3.3)$$

The proposed feedback scheme is illustrated in Figure 3.1. Letting  $D \triangleq$

<sup>†</sup>In contrast to the droop-control literature, for the moment we make no assumptions regarding the selection of the droop coefficients. In Section 3.1, we will see that there is a particular selection of coefficients which leads to desirable steady-state power sharing properties for the closed-loop system.

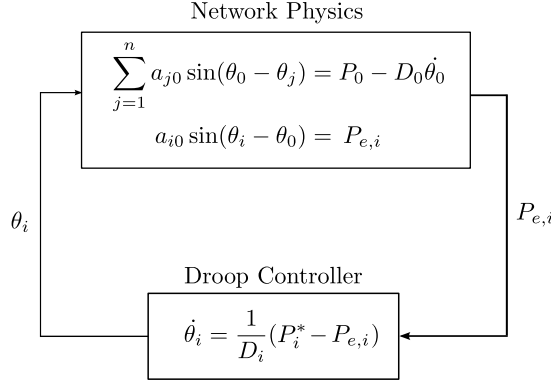


FIG. 3.1. Feedback loop for the frequency-droop controller.

$\text{diag}(0, D_1, \dots, D_n)$ ,  $P^* \triangleq (P_0^*, P_1^*, \dots, P_n^*)^T$ , for  $i \in \{1, \dots, n\}$  writing  $a_{i0} \triangleq E_i E_0 |Y_{i0}|$ , and finally using (2.1) we obtain in vector notation

$$D\dot{\theta} = P^* - B\text{diag}(\{a_{i0}\}_{i=1}^n)\mathbf{sin}(B^T\theta). \quad (3.4)$$

Augmenting (3.3) with an additional frequency-dependent load  $D_0\dot{\theta}_0$ , the closed-loop frequency-droop controlled system (3.4) (or equivalently (3.2) and (3.3) in components) is seen to be in exact correspondance with a network of *multi-rate Kuramoto oscillators* similar to those described in (1.1). The prefix “multi-rate” refers to the heterogeneous time constants  $D_i$  which regulate the individual speeds of the oscillators. One can interpret the constant power load case of (3.4) with  $D_0 = 0$  as the limit of the phase oscillator at the load becoming extremely fast as  $D_0 \rightarrow 0^+$  [37]. We summarize the above discussion in Theorem 3.1, the proof of which is immediate.

**THEOREM 3.1 (Droop-controlled inverters are Kuramoto oscillators).**

Consider the parallel microgrid depicted in Figure 1.1. The following two statements are equivalent:

- (i) each inverter is controlled according to the frequency-droop method (3.1) and the electrical network obeys the active power flow equations (1.3);
- (ii) the closed-loop system is a network of multi-rate Kuramoto oscillators described by (3.4), with rate constants  $D_i$ , natural frequencies  $P_i^*$ , node-edge incidence matrix  $B$  given by (2.1) and edge weights  $a_{i0}$ .

There are several insightful ways to interpret the action of the control law (3.1).

**REMARK 3.2 (Interpretation of frequency-droop controller).**

- (i) Figure 3.1 suggests the following simple interpretation of the controller (3.1); modify phase angle at each inverter according to whether the nominal power value  $P_i^*$  balances the active power demand  $P_{e,i}$  or not. The hope is then that the state  $\theta \in \mathbb{T}^{n+1}$  evolves towards a stable root of the load flow (1.3). The method therefore specifies a continuous version of the Newton-Raphson iteration, as used in the field of dynamic optimization [38].
- (ii) A rearrangement of (3.1) shows that the controller specifies the total power injection at each inverter as the sum of a constant power injection  $P_i^*$  and a frequency dependent power injection  $-D_i\dot{\theta}_i$ . It is this frequency-dependent term which specifies the difference in power between the nominal and necessary power injections. The controller is therefore a structure preserving controller, in the sense of [37].



A natural question now arises: under what conditions on the power injections, network admittances, and droop coefficients does the closed-loop system (3.4) possess a stable, synchronous solution? The following result provides a definitive answer and characterizes some important properties of the solution.

**THEOREM 3.3 (Existence and Stability of Sync'd Solution).** *Consider the frequency-droop controlled system (3.4), and define the scaled power imbalance  $\omega_{\text{avg}}$  by  $\omega_{\text{avg}} \triangleq (\sum_{i=0}^n P_i^*) / (\sum_{i=1}^n D_i) \in \mathbb{R}$ . The following two statements are equivalent:*

- (i) **Synchronization:** *There exists an arc length  $\gamma \in [0, \pi/2)$  such that the system (3.4) possess a locally exponentially stable and unique synchronized solution  $t \mapsto \theta^*(t) \in \overline{\Delta}_G(\gamma)$  for all  $t \geq 0$ ;*
- (ii) **Parametric condition:**

$$\Gamma \triangleq \max_{i \in \{1, \dots, n\}} |(P_i^* - \omega_{\text{avg}} D_i) / a_{i0}| < 1. \quad (3.5)$$

If the equivalent statements (i) and (ii) hold true, then the quantities  $\Gamma$  and  $\gamma \in [0, \pi/2)$  are related uniquely via  $\Gamma = \sin(\gamma)$ , and following statements hold:

- a) **Explicit synchronized solution and frequency:** *the synchronized solution satisfies  $\theta^*(t) = (\theta_0 + \omega_{\text{sync}} t \mathbf{1}_{n+1}) \pmod{2\pi}$  for some  $\theta_0 \in \overline{\Delta}_G(\gamma)$ , where  $\omega_{\text{sync}} = \omega_{\text{avg}}$ , and the synchronized angular differences satisfy  $\sin(\theta_i^* - \theta_0^*) = (P_i^* - \omega_{\text{sync}} D_i) / a_{i0}$ ,  $i \in \{1, \dots, n\}$ ;*
- b) **Explicit synchronization rate:** *The local exponential synchronization rate is no worse than*

$$\lambda \triangleq \frac{\lambda_2(L(a_{i0}))}{\max_{i \in \{1, \dots, n\}} D_i} \sqrt{1 - \Gamma^2}. \quad (3.6)$$

**REMARK 3.4 (Physical interpretation and comments).** *From Remark 3.2 (ii), it is clear that  $P_i^* - \omega_{\text{sync}} D_i$  is the steady-state power injection at the  $i^{\text{th}}$  inverter. In addition, we noted earlier that  $a_{i0} = E_i E_0 |Y_{i0}|$  is the physical active power transfer limit along the line  $\{i, 0\} \in \mathcal{E}$ . Physically, the parametric condition (3.5) therefore states that the active power injection at each inverter be feasible. In this sense, the stability of the overall system decouples into the stability of individual inverters. Theorem 3.3 shows that equilibrium power flows are invariant under constant scaling of all droop coefficients, as overall scaling of  $D$  appears inversely in  $\omega_{\text{avg}}$ . In the proof we show that without loss of generality, we can place ourselves in an appropriate rotating frame in which the necessary and sufficient condition (ii) reads that  $\max_{i \in \{1, \dots, n\}} |\tilde{P}_i / a_{i0}| < 1$ , for some appropriately defined values  $\tilde{P}_i$ . The **existence** of an exponentially stable synchronized solution is therefore completely independent of the selected droop coefficient values. Namely, if a synchronized solution exists for one selection of droop coefficients, a synchronized solution (albeit different) will exist for any other selection.*

*Proof.* To begin, note that if a solution  $t \mapsto \theta(t)$  to the system (3.4) is frequency synchronized, then by definition there exists an  $\omega_{\text{sync}} \in \mathbb{R}$  such that  $\dot{\theta}(t) = \omega_{\text{sync}} \mathbf{1}_{n+1}$  for all  $t \geq 0$ . Summing over all equations (3.2)–(3.3) then gives that  $\omega_{\text{sync}} = \omega_{\text{avg}}$ . We now present a definition to facilitate the proof of our stability results. Without loss of generality, we can consider the *auxiliary system* associated with (3.4) defined by

$$D\dot{\theta} = \tilde{P} - B \text{diag}(\{a_{i0}\}_{i=1}^n) \mathbf{sin}(B^T \theta), \quad (3.7)$$



where  $\tilde{P}_i = P_i^* - \omega_{\text{avg}} D_i$ ,  $i \in \{1, \dots, n\}$  and  $\tilde{P}_0 = P_0^*$ . The auxiliary system has the property that  $\tilde{\omega}_{\text{avg}} = \sum_{i=0}^n \tilde{P}_i / \sum_{i=1}^n D_i = 0$ , and represents the dynamics (3.4) in a reference rotating at an angular frequency  $\omega_{\text{avg}}$ . Thus, frequency synchronized solutions of (3.4) with synchronization frequency  $\omega_{\text{avg}}$  correspond to equilibrium points of the system (3.7) and vice versa. Given the Laplacian matrix  $L = B \text{diag}(\{a_{i0}\}_{i=1}^n) B^T$  of the network, equation (3.7) can be equivalently rewritten in the insightful form

$$D\dot{\theta} = B \text{diag}(\{a_{i0}\}_{i=1}^n) \cdot (B^T L^\dagger \tilde{P} - \mathbf{sin}(B^T \theta)). \quad (3.8)$$

Here we have made use of the facts that  $L \cdot L^\dagger = L^\dagger \cdot L = I_{n+1} - \frac{1}{n+1} \mathbf{1}_{n+1} \mathbf{1}_{n+1}^T$  (follows from the singular value decomposition [39]) and  $\mathbf{1}_{n+1}^T \tilde{P} = 0$  (due to power balancing  $\sum_{i=0}^n \tilde{P}_i = 0$  in the rotating frame). For an acyclic graph, it is known that [40, Theorem 3.5, (G1)] for any  $\gamma \in [0, \pi/2)$ , the right-hand side of (3.8) admits a unique and locally exponentially stable<sup>¶</sup> equilibrium  $\theta^* \in \bar{\Delta}_G(\gamma)$  if and only if  $\|B^T L^\dagger \tilde{P}\|_\infty \leq \sin(\gamma)$ .

For the given (acyclic) star topology, one can verify by direct calculation that the  $i^{\text{th}}$  element of the vector  $B^T L^\dagger \tilde{P} \in \mathbb{R}^n$  is exactly  $\tilde{P}_i/a_{i0}$ , the ratio of the power injection at the  $i^{\text{th}}$  inverter to the maximum power transfer between the  $i^{\text{th}}$  inverter and the load. We therefore have that for any  $\gamma \in [0, \pi/2)$ , the necessary and sufficient condition  $\|B^T L^\dagger \tilde{P}\|_\infty \leq \sin(\gamma)$  becomes  $\Gamma \triangleq \max_{i \in \{1, \dots, n\}} \tilde{P}_i/a_{i0} \leq \sin(\gamma)$ . Since the right-hand side of the condition  $\Gamma \leq \sin(\gamma)$  is a concave function of  $\gamma \in [0, \pi/2)$ , there exists an equilibrium  $\theta^* \in \bar{\Delta}_G(\gamma)$  for some  $\gamma \in [0, \pi/2)$  if and only if the condition  $\Gamma \leq \sin(\gamma)$  is true with the strict inequality sign for  $\gamma = \pi/2$ . This leads immediately to the condition that  $\Gamma < 1$ , as claimed. Additionally, if  $\Gamma = \sin(\gamma)$  for some  $\gamma \in [0, \pi/2)$ , then the explicit equilibrium angles are obtained from the  $n$  decoupled equations  $B^T L^\dagger \tilde{P} = \mathbf{sin}(B^T \theta^*)$ . In summary, the above discussion shows (in the original non-rotating coordinates) the equivalence of (i) and (ii) and statement (a).

To show statement (b), we consider the Jacobian matrix of the dynamics (3.7) at the exponentially stable fixed point, given by

$$J(\theta^*) = -D^{-1} B \text{diag}(\{a_{i0} \cos(\theta_i^* - \theta_0^*)\}_{i=1}^n) B^T = -D^{-1} L(\theta^*).$$

The matrix  $L(\theta^*)$  is positive semidefinite, with a simple eigenvalue at zero corresponding to rotational invariance of the dynamics under a uniform shift of all angles. We will now attempt to bound from below the second smallest eigenvalue of  $D^{-1} L(\theta^*)$ , and thus give a worst case estimate of the local convergence rate of (3.7) to the stable equilibrium  $\theta^* \in \bar{\Delta}_G(\gamma)$ . A simple bound can be obtained via the *Courant-Fischer Theorem* [42], which states for any real symmetric matrix  $M \in \mathbb{R}^{n \times n}$  that

$$\lambda_{\min}(M) = \min_{x \in \mathbb{R}^n} \frac{x^T M x}{x^T x}.$$

To begin, for  $x \in \mathbb{R}^n$  let  $y = D^{\frac{1}{2}} x$ , and note that

$$\frac{y^T D^{-\frac{1}{2}} L(\theta^*) D^{-\frac{1}{2}} y}{y^T y} = \frac{x^T L(\theta^*) x}{x^T D x}.$$

<sup>¶</sup> The stability property proved in [40] applies, strictly speaking, only to pure differential equations. However, it is well known that a locally exponentially stable equilibrium  $\theta^* \in \bar{\Delta}_G(\pi/2)$  of the differential-algebraic system (3.8) with  $D_0 = 0$  has the same local stability properties as the identical equilibrium  $\theta^*$  of the corresponding system of pure differential equations with  $D_0 > 0$ , see [41].

Note that  $y \in \mathbb{R}^n$  is a normalized eigenvector of  $D^{-\frac{1}{2}}L(\theta^*)D^{-\frac{1}{2}}$  with eigenvalue  $\mu \in \mathbb{R}$  if and only if  $x = D^{-\frac{1}{2}}y$  is an eigenvector of  $D^{-1}L(\theta^*)$  with the same eigenvalue. Letting  $y \in \mathbb{R}^n$  be an arbitrary nonzero vector in the subspace orthogonal to  $\mathbf{1}_{n+1}$ , we have that

$$\begin{aligned} \lambda_2(D^{-1}L(\theta^*)) &= \min_{y \in \mathbb{R}^n} \frac{y^T D^{-\frac{1}{2}}L(\theta^*)D^{-\frac{1}{2}}y}{y^T y} = \min_{x \in \mathbb{R}^n} \frac{x^T L(\theta^*)x}{x^T D x} \\ &\geq \frac{1}{\max_{i \in \{1, \dots, n\}} D_i} \min_{x \in \mathbb{R}^n} \frac{x^T L(\theta^*)x}{x^T x} \\ &\geq \frac{\lambda_2(L(\theta^*))}{\max_{i \in \{1, \dots, n\}} D_i}. \end{aligned}$$

Since  $\theta^* \in \overline{\Delta}_G(\gamma)$ , the eigenvalue  $\lambda_2(L(\theta^*))$  can be further bounded as  $\lambda_2(L(\theta^*)) \geq \lambda_2(L(a_{i0})) \cos(\gamma)$ , where  $L(a_{i0}) = B \text{diag}(\{a_{i0}\}_{i=1}^n) B^T$  is the Laplacian matrix with weights  $\{a_{i0}\}_{i=1}^n$ . Combining this with the identity  $\cos(\sin^{-1}(z)) = \sqrt{1 - z^2}$  for  $z \in \mathbb{R}$  suffices to show the result.  $\square$

**3.1. Selection of Droop Coefficients and Actuation Constraints.** Theorem 3.3 gives us a necessary and sufficient condition for the existence of a synchronized solution of (3.4). However, the result offers no immediate guidance on how to properly select the droop coefficients. Indeed, we will see that an improper selection of droop coefficients can lead to behaviour which, for any choice of  $P_i^* \in [0, \overline{P}_i]$ , violates the actuation constraint  $P_{e,i} \in [0, \overline{P}_i]$  of Section 2. In addition, although rearranging the condition (3.5) of Theorem 3.3 gives us a bound on the allowable load  $P_0^*$  for any particular choices of  $\{P_i^*\}_{i=1}^n$ , this bound is somewhat complicated, and does not take into account the underlying additional constraint that  $P_0^* \leq 0$ .

We now present a definition which characterizes the ‘‘proper’’ way to select the droop coefficients. We then show that if one selects the droop coefficients according to this definition, the resulting behaviour of the steady-state power flow satisfies the actuation constraints. The result also gives a bound on the magnitude of the allowable load that can be serviced without violating these power injection constraints.

**DEFINITION 3.5 (Proportional Droop Coefficients).** *The droop coefficients are said to be selected proportionally if for each  $i, j \in \{1, \dots, n\}$ ,*

$$\frac{P_i^*}{D_i} = \frac{P_j^*}{D_j}. \quad (3.9)$$

**LEMMA 3.6 (Power Flow Constraints and Power Sharing).** *Consider a synchronized solution the frequency-droop controlled system (3.4), and let the droop coefficients be selected proportionally according to Definition 3.5. The following two statements are equivalent:*

- (i) **Power flow constraints:**  $0 \leq P_{e,i} \leq \overline{P}_i, \quad i \in \{1, \dots, n\};$
- (ii) **Load constraints:**  $-\left(\min_{i \in \{1, \dots, n\}} \frac{\overline{P}_i}{P_i^*}\right) \cdot \sum_{j=1}^n P_j^* \leq P_0^* \leq 0.$

Moreover, the inverters share the load  $P_0^*$  proportionally according to their power ratings (that is,  $P_{e,i}/\overline{P}_i = P_{e,j}/\overline{P}_j, i, j \in \{1, \dots, n\}$ ) if and only if  $P_i^* = \overline{P}_i$  for each inverter.

*Proof.* In synchronous steady state, we have that  $\dot{\theta}_i = \omega_{\text{sync}} = (P_0^* + \sum_{i=1}^n P_i^*) / (\sum_{i=1}^n D_i)$  for each  $i \in \{0, \dots, n\}$ . Substituting this in (3.2), we see that the steady-state active power injection at each inverter is given by  $P_{e,i} = a_{i0} \sin(\theta_i^* - \theta_0^*) =$

$P_i^* - \omega_{\text{sync}} D_i$ . By imposing for each  $i \in \{1, \dots, n\}$  that  $P_{e,i} \geq 0$ , substituting the expression for  $\omega_{\text{sync}}$ , and rearranging terms, we calculate for each  $i \in \{1, \dots, n\}$  that

$$P_{e,i} = P_i^* - \left( \frac{P_0^* + \sum_{j=1}^n P_j^*}{\sum_{j=1}^n D_j} \right) D_i \geq 0 \iff P_0^* \leq - \sum_{j=1}^n \left( P_j^* - \frac{P_i^*}{D_i} D_j \right) = 0,$$

where in the final equality we have made use of the proportional selection of droop coefficients given by (3.9). This suffices to show half of the inequalities in the equivalence of (i) and (ii). If we now impose that  $P_{e,i} \leq \bar{P}_i$  and again use the expression for  $\omega_{\text{sync}}$  along with (3.9), a similar calculation to that above gives that

$$\begin{aligned} P_{e,i} \leq \bar{P}_i &\iff P_0^* \geq - \frac{\bar{P}_i}{P_i^*} \sum_{j=1}^n P_j^*, \quad i \in \{1, \dots, n\}, \\ &\iff P_0^* \geq - \left( \min_{i \in \{1, \dots, n\}} \frac{\bar{P}_i}{P_i^*} \right) \sum_{j=1}^n P_j^*, \end{aligned}$$

which shows the remaining inequalities in the equivalence of (i) and (ii). To show the final statement, we select each  $P_i^*$  to be equal to  $\bar{P}_i$  and note that the fraction of the rated power capacity consumed by the  $i^{\text{th}}$  inverter is given by

$$\frac{P_{e,i}}{\bar{P}_i} = \frac{\bar{P}_i - \omega_{\text{sync}} D_i}{\bar{P}_i} = 1 - \omega_{\text{sync}} \frac{D_i}{\bar{P}_i} = 1 - \omega_{\text{sync}} \frac{D_j}{\bar{P}_j} = \frac{\bar{P}_j - \omega_{\text{sync}} D_j}{\bar{P}_j} = \frac{P_{e,j}}{\bar{P}_j},$$

for each  $j \in \{1, \dots, n\}$ . This completes the proof.  $\square$

The final statement of Lemma 3.6 is the frequently cited *coefficient matching* condition of the microgrid/droop control literature. Note in particular that the coefficients  $D_i$  must be selected with global knowledge. The droop method therefore requires a centralized design for power sharing despite its distributed implementation, and does not allow for plug-and-play power sharing functionality without the global recomputation of all coefficients. Lemma 3.6 holds independent of the voltage magnitudes at each inverter, and independent of the network susceptance values.

**3.2. Adaptive Droop Controller for Frequency Regulation.** As is evident from the expression for  $\omega_{\text{sync}}$  in Theorem 3.3, the frequency-droop method typically leads to a deviation of the steady-state operating frequency  $\omega_0 + \omega_{\text{sync}}$  from the nominal value  $\omega_0$ . Again in light of Theorem 3.3, it is clear that modifying the nominal active power injection  $P_i^*$  via the transformation  $P_i^* \rightarrow P_i^* - \omega_{\text{sync}} D_i$  in (3.2) will yield zero steady-state frequency deviation (c.f. the auxiliary system (3.7) with  $\tilde{\omega}_{\text{sync}} = 0$ ). Unfortunately, each inverter does not immediately have access to the value  $\omega_{\text{sync}}$  for use in such a control procedure. There are two ways to view the difficulty in proceeding:

- (i) although the information to immediately calculate  $\omega_{\text{sync}}$  is available (namely all  $P_i^*$ , including the network load  $P_0^*$ , and all  $D_i$  values), this information is distributed throughout the network and therefore not locally available to each inverter;
- (ii) as originally proposed in [2], after the frequency of each inverter has converged to  $\omega_{\text{sync}}$ , a slower, secondary control loop can be used locally at each inverter. Each local secondary control loop restores the frequency of the corresponding inverter to its nominal value  $\omega_0$  by slowly modifying the nominal

power injection  $P_i^*$  until the network frequency deviation is zero. This procedure implicitly assumes that the measured frequency value  $\hat{\theta}_i(t)$  is a good approximation of  $\omega_{\text{sync}}$ , and relies on a separation of time scales between the fast, synchronization-enforcing primary droop controller and the slower secondary controller. This methodology is explained in [2, 43] and [11]. We note that this approach can become particularly slow if the droop coefficients are selected to be quite large, since in this case Theorem 3.3 (b) shows that the required separation in time scales may be quite large. Moreover, this slow response leads to an inability of the method to dynamically regulate the frequency to a nominal value in the presence of a time-varying load.

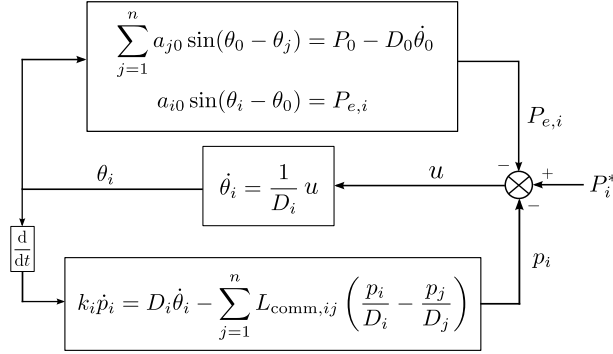


FIG. 3.2. Feedback diagram for regulation of nominal frequency in droop-controlled microgrid. The secondary control loop containing  $p_i$  can be thought of as dynamically implementing the coordinate change  $P_i^* \rightarrow P_i^* - \omega_{\text{sync}} D_i$  as in (3.7).

In the sequel we will pursue an alternative scheme for frequency restoration which does not implicitly rely on a separation of time-scales as in [2, 43] and [11]. The price we pay for this relaxation is the requirement of a sparse communication network between the inverters<sup>†</sup>. However, in contrast to the previous techniques, the currently proposed controller is able to dynamically regulate the network frequency in the presence of a time-varying load. We expand on the conventional frequency droop design (1.2) and propose the *adaptive droop controller*

$$D_i \dot{\theta}_i = P_i^* - p_i - P_{e,i}, \quad i \in \{1, \dots, n\}, \quad (3.10)$$

$$k_i \dot{p}_i = D_i \dot{\theta}_i - \sum_{j=1}^n L_{\text{comm},ij} \left( \frac{p_i}{D_i} - \frac{p_j}{D_j} \right), \quad i \in \{1, \dots, n\}, \quad (3.11)$$

where  $p_i \in \mathbb{R}$  and  $k_i > 0$  for each  $i \in \{1, \dots, n\}$ . The matrix  $L_{\text{comm}} \in \mathbb{R}^{n \times n}$  is the Laplacian matrix corresponding to a weighted, undirected and connected *communication graph*  $G_{\text{comm}} = (\mathcal{V}_{\text{comm}}, \mathcal{E}_{\text{comm}}, L_{\text{comm}})$  between the inverters. The only requirement on the weighted, undirected graph  $G_{\text{comm}}$  is that it be connected.

This control methodology is depicted in Figure 3.2. The intuition of the adaptive droop controller (3.10)–(3.11) can be revealed by considering first the case where  $L_{\text{comm}}$  is identically zero. In this case, from (3.11) we can write for each  $i \in \{1, \dots, n\}$

<sup>†</sup>Although we here examine the case of continuous time communication among the inverters, the presented results extend to discrete time and asynchronous communication, see [21] for further details.

that  $p_i(t) = k_i^{-1} D_i \int_0^t \dot{\theta}_i(\tau) d\tau$ . Substituting this into (3.10) we have that

$$P_{e,i} = P_i^* - D_i \dot{\theta}_i - k_i^{-1} D_i \int_0^t \dot{\theta}_i d\tau,$$

which can be interpreted as a proportional-integral (PI) frequency controller (see Remark 3.2). The additional consensus term  $L_{\text{comm}}$  is needed in the controller (3.11) such that  $p_i/D_i = \omega_{\text{avg}} = \sum_{j=0}^n P_j^* / \sum_{j=1}^n D_j$  becomes identical for all inverters. In essence, the controller (3.10)–(3.11) enforces the desired rotating frame coordinate transformation  $p_i \rightarrow \omega_{\text{avg}} D_i$  in a distributed manner. The closed-loop dynamical system resulting from the adaptive droop controller (3.10)–(3.11) is given by

$$D_i \dot{\theta}_i = P_i^* - p_i - a_{i0} \sin(\theta_i - \theta_0), \quad i \in \{1, \dots, n\}, \quad (3.12)$$

$$0 = P_0^* - \sum_{j=1}^n a_{0j} \sin(\theta_0 - \theta_j) \quad (3.13)$$

$$k_i \dot{p}_i = P_i^* - p_i - a_{i0} \sin(\theta_i - \theta_0) - \sum_{j=1}^n L_{\text{comm},ij} \left( \frac{p_i}{D_i} - \frac{p_j}{D_j} \right), \quad i \in \{1, \dots, n\}. \quad (3.14)$$

The following Theorem establishes a local stability result which holds independently from the choice of the particular controller parameters  $P_i^* \in [0, \bar{P}_i]$ ,  $D_i > 0$ ,  $k_i > 0$  for  $i \in \{1, \dots, n\}$  and  $L_{\text{comm}} \in \mathbb{R}^{n \times n}$ , as long as the droop control stability condition (3.5) of Theorem 3.6 holds true. In effect, the following result states that if the original droop controller (3.1) succeeds in stabilizing the network, then so does the adaptive droop controller (3.10)–(3.11).

**THEOREM 3.7 (Stability of Adaptive Droop Controller).** *Consider the closed-loop system (3.12)–(3.14) resulting from the adaptive droop controller (3.10)–(3.11) with parameters  $P_i^* \in (0, \bar{P}_i]$ ,  $D_i > 0$  and  $k_i > 0$  for  $i \in \{1, \dots, n\}$ , and connected communication Laplacian  $L_{\text{comm}} \in \mathbb{R}^{n \times n}$ . The following two statements are equivalent:*

- (i) **Parametric Condition:** *The droop control stability condition (3.5) holds;*
- (ii) **Stability of Adaptive Controller:** *There exists an arc length  $\gamma \in [0, \pi/2)$  such that the system (3.12)–(3.14) possess a locally exponentially stable and unique equilibrium  $(\theta^*, p^*) \in \bar{\Delta}_G(\gamma) \times \mathbb{R}^n$ .*

*If the equivalent statements (i) and (ii) hold true, then the unique equilibrium is given by  $\sin(\theta_i^* - \theta_0^*) = (P_i^* - \omega_{\text{avg}} D_i) / a_{i0}$ ,  $p_i^* = D_i \omega_{\text{avg}}$  for  $i \in \{1, \dots, n\}$ .*

*Proof.* See Appendix A. □

**3.3. Simulation of Adaptive Droop System.** In order to validate the adaptive droop controller (3.10)–(3.11) and to illustrate its effectiveness, we now present a simulation study, where  $n = 5$  inverters operating in parallel are controlled according to the adaptive droop law. We simulate a structure-preserving model for the load with  $D_0 = 0.1 \text{ W} \cdot \text{s}$ . The remaining simulation parameters are detailed in Table 3.1 and the simulation results are displayed in Figure 3.3.

The microgrid dynamics are initiated in synchronous steady-state supplying a load of 5 kW, with the load increasing instantaneously to 10 kW at  $t = 2 \text{ s}$ . The frequency spiking behaviour displayed Figure 3.3 (c) arises from the instantaneous change in load, and not from second-order dynamics associated with the addition of the secondary controller. Conversely, the fast dynamics of the auxiliary variable  $p$  in Figure 3.3 (d) is entirely due to the small values of  $k_i$  used in the simulation.

Note the effectiveness of the adaptive droop controller in quickly regulating the system frequency to the nominal value. The system frequency is kept within  $\simeq 0.15\text{Hz}$  of the nominal, with a selection of droop coefficients much smaller than is typical in the literature ( $10^3$ , compared to roughly  $10^5$ ). This selection of smaller droop coefficients allows for the inverters to respond more quickly during transients. In contrast to the existing literature, we therefore see that it is possible to implement a fast secondary control loop while providing frequency regulation in the presence of extreme load variation.

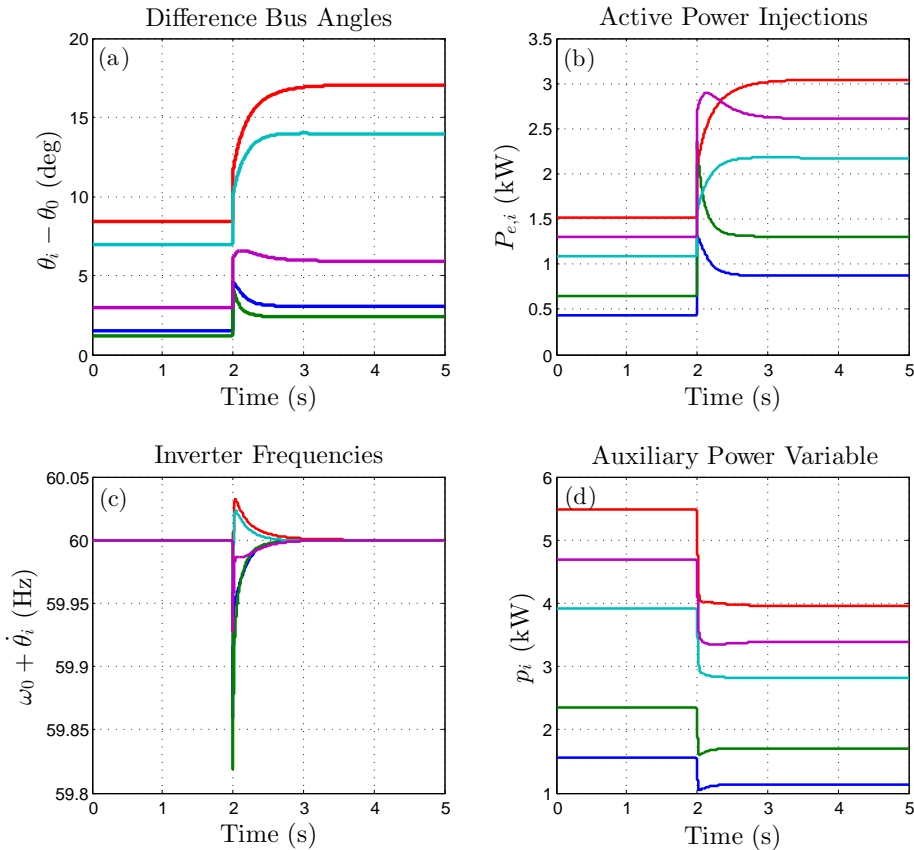


FIG. 3.3. Simulation of the adaptive droop controlled closed-loop (3.12)–(3.14).

**4. Conclusions.** Leveraging recent results from the theory of coupled oscillators and from classical power systems, we have presented the first nonlinear analysis of the frequency-droop controller. In addition, we have proposed and analyzed a secondary controller with dynamically regulates the system frequency to a nominal value in the presence of a time-varying load. Works to follow will extend this analysis to reactive power sharing and to networks with non-zero transfer conductances.

**References.**

[1] A. Mohd, E. Ortjohann, D. Morton, and O. Omari. Review of control techniques

TABLE 3.1

Parameter values for simulation of paralleled microgrid under the adaptive droop controller.

Parameter	Symbol	Value
Nominal Frequency	$\omega_0/2\pi$	60 Hz
Output/Line Inductances	$-1/b_{i0}\omega_0$	[20, 10, 30, 35, 13] mH
Inverter Output Voltages	$E_i$	[363, 350, 345, 350, 365] V
Load Voltage	$E_0$	340 V
Inverter Ratings	$P_i^* = \bar{P}_i$	[2, 3, 7, 5, 6] kW
Load	$P_0^*(t)$	$-5\text{kW} - 5\text{kW} \cdot \text{Heaviside}(t - 2\text{s})$
Droop Coefficients	$D_i$	$[1, 1.5, 3.5, 2.5, 3] \times 10^3 \text{ W} \cdot \text{s}$
Auxiliary Droop Coeffiencts	$k_i$	$10^{-2} \text{ s}$
Communication Graph	$G_{\text{comm}}$	Linear Graph Between Inverters
Communication Laplacian	$L_{\text{comm}}$	$HH^T \times 10^4 \text{ W} \cdot \text{s}$
	$H \in \mathbb{R}^{n \times (n-1)}$	$H_{ij} = 1$ if $i = j$ , $H_{ij} = -1$ if $i = j + 1$ , else zero.

for inverters parallel operation. *Electric Power Systems Research*, 80(12):1477 – 1487, 2010.

- [2] M. C. Chandorkar, D. M. Divan, and R. Adapa. Control of parallel connected inverters in standalone AC supply systems. *IEEE Transactions on Industry Applications*, 29(1):136–143, 1993.
- [3] P. Kundur. *Power System Stability and Control*. McGraw-Hill, 1994.
- [4] J. M. Guerrero, L. Garcia de Vicuna, J. Matas, M. Castilla, and J. Miret. Output impedance design of parallel-connected UPS inverters with wireless load-sharing control. *IEEE Transactions on Industrial Electronics*, 52(4):1126–1135, 2005.
- [5] W. Yao, M. Chen, J. Matas, J. M. Guerrero, and Z.-M. Qian. Design and analysis of the droop control method for parallel inverters considering the impact of the complex impedance on the power sharing. *IEEE Transactions on Industrial Electronics*, 58(2):576–588, 2011.
- [6] A. Tuladhar, H. Jin, T. Unger, and K. Mauch. Parallel operation of single phase inverter modules with no control interconnections. In *Applied Power Electronics Conference and Exposition*, volume 1, pages 94–100, February 1997.
- [7] S. Barsali, M. Ceraolo, P. Pelacchi, and D. Poli. Control techniques of dispersed generators to improve the continuity of electricity supply. In *IEEE Power Engineering Society Winter Meeting*, volume 2, pages 789–794, 2002.
- [8] J. A. P. Lopes, C. L. Moreira, and A. G. Madureira. Defining control strategies for microgrids islanded operation. *IEEE Transactions on Power Systems*, 21(2):916–924, 2006.
- [9] R. Majumder, A. Ghosh, G. Ledwich, and F. Zare. Power system stability and load sharing in distributed generation. In *Power System Technology and IEEE Power India Conference*, pages 1–6, New Delhi, India, October 2008.
- [10] Y.U. Li and C.-N. Kao. An accurate power control strategy for power-electronics-interfaced distributed generation units operating in a low-voltage multibus microgrid. *IEEE Transactions on Power Electronics*, 24(12):2977–2988, 2009.
- [11] J. M. Guerrero, J. C. Vasquez, J. Matas, M. Castilla, and L. G. de Vicuna. Control strategy for flexible microgrid based on parallel line-interactive UPS systems. *IEEE Transactions on Industrial Electronics*, 56(3):726–736, 2009.



- [12] E.A.A. Coelho, P.C. Cortizo, and P.F.D. Garcia. Small-signal stability for parallel-connected inverters in stand-alone AC supply systems. *IEEE Transactions on Industry Applications*, 38(2):533–542, 2002.
- [13] M. Dai, M. N. Marwali, J.-W. Jung, and A. Keyhani. Power flow control of a single distributed generation unit with nonlinear local load. In *IEEE Power Systems Conference and Exposition*, pages 398–403, October 2004.
- [14] M. N. Marwali, J.-W. Jung, and A. Keyhani. Stability analysis of load sharing control for distributed generation systems. *IEEE Transactions on Energy Conversion*, 22(3):737–745, 2007.
- [15] Y. Mohamed and E. F. El-Saadany. Adaptive decentralized droop controller to preserve power sharing stability of paralleled inverters in distributed generation microgrids. *IEEE Transactions on Power Electronics*, 23(6):2806–2816, 2008.
- [16] R. Majumder, A. Ghosh, G. Ledwich, and F. Zare. Angle droop versus frequency droop in a voltage source converter based autonomous microgrid. In *IEEE Power Energy Society General Meeting*, pages 1–8, July 2009.
- [17] Q.-C. Zhong. Robust droop controller for accurate proportional load sharing among inverters operated in parallel. *IEEE Transactions on Industrial Electronics*, 2011. To appear.
- [18] Q.-C. Zhong and G. Weiss. Synchronverters: Inverters that mimic synchronous generators. *IEEE Transactions on Industrial Electronics*, 58(4):1259–1267, 2011.
- [19] R. Olfati-Saber, J. A. Fax, and R. M. Murray. Consensus and cooperation in networked multi-agent systems. *Proceedings of the IEEE*, 95(1):215–233, 2007.
- [20] W. Ren, R. W. Beard, and E. M. Atkins. A survey of consensus problems in multi-agent coordination. In *American Control Conference*, pages 1859–1864, Portland, OR, June 2005.
- [21] F. Bullo, J. Cortés, and S. Martínez. *Distributed Control of Robotic Networks*. Applied Mathematics Series. Princeton University Press, 2009. Available at <http://www.coordinationbook.info>.
- [22] L.A.B Tórres, J.P. Hespanha, and J. Moehlis. Power supplies dynamical synchronization without communication. November 2011. Submitted to conference.
- [23] S. Bolognani and S. Zampieri. A distributed control strategy for reactive power compensation in smart microgrids. *Arxiv preprint arXiv:1106.5626v2*, 2011.
- [24] H. Xin, Z. Qu, J. Seuss, and A. Maknouninejad. A self organizing strategy for power flow control of photovoltaic generators in a distribution network. *Power Electronics, IEEE Transactions on*, 26(3):1462–1473, August 2011.
- [25] Y. Kuramoto. Self-entrainment of a population of coupled non-linear oscillators. In H. Araki, editor, *Int. Symposium on Mathematical Problems in Theoretical Physics*, volume 39 of *Lecture Notes in Physics*, pages 420–422. Springer, 1975.
- [26] S. H. Strogatz. Exploring complex networks. *Nature*, 410(6825):268–276, 2001.
- [27] S. Boccaletti, V. Latora, Y. Moreno, M. Chavez, and D. U. Hwang. Complex networks: Structure and dynamics. *Physics Reports*, 424(4-5):175–308, 2006.
- [28] A. Arenas, A. Díaz-Guilera, J. Kurths, Y. Moreno, and C. Zhou. Synchronization in complex networks. *Physics Reports*, 469(3):93–153, 2008.
- [29] S. H. Strogatz. From Kuramoto to Crawford: Exploring the onset of synchronization in populations of coupled oscillators. *Physica D: Nonlinear Phenomena*, 143(1):1–20, 2000.
- [30] F. Dörfler and F. Bullo. On the critical coupling for Kuramoto oscillators. *SIAM Journal on Applied Dynamical Systems*, 10(3):1070–1099, 2011.
- [31] J. A. Acebrón, L. L. Bonilla, C. J. P. Vicente, F. Ritort, and R. Spigler. The

- Kuramoto model: A simple paradigm for synchronization phenomena. *Reviews of Modern Physics*, 77(1):137–185, 2005.
- [32] F. Dörfler and F. Bullo. Exploring synchronization in complex oscillator networks. In *IEEE Conf. on Decision and Control*, Maui, HI, USA, December 2012. Submitted.
- [33] E. C. Furtado, L. A. Aguirre, and L. A. B. Tôrres. UPS parallel balanced operation without explicit estimation of reactive power – a simpler scheme. *IEEE Transactions on Circuits and Systems II: Express Briefs*, 55(10):1061–1065, 2008.
- [34] G. Weiss, Q.-C. Zhong, T. C. Green, and J. Liang.  $H^\infty$  repetitive control of DC-AC converters in microgrids. *IEEE Transactions on Power Electronics*, 19(1):219–230, 2004.
- [35] T. Hornikand and Q.-C. Zhong. A current-control strategy for voltage-source inverters in microgrids based on  $H^\infty$  and repetitive control. *IEEE Transactions on Power Electronics*, 26(3):943–952, 2011.
- [36] B. W. Williams. *Power Electronics: Devices, Drivers, Applications and Passive Components*. Mcgraw-Hill, 1992.
- [37] A. R. Bergen and D. J. Hill. A structure preserving model for power system stability analysis. *IEEE Transactions on Power Apparatus and Systems*, 100(1):25–35, 1981.
- [38] A.E. Bryson. *Dynamic Optimization*. Texts in Applied Mathematics. Addison-Wesley, 1999.
- [39] F. Dörfler and F. Bullo. Kron reduction of graphs with applications to electrical networks. *IEEE Transactions on Circuits and Systems*, November 2011. To appear.
- [40] F. Dörfler, M. Chertkov, and F. Bullo. Synchronization in complex oscillator networks and smart grids. May 2012. Submitted.
- [41] S. Sastry and P. Varaiya. Hierarchical stability and alert state steering control of interconnected power systems. *IEEE Transactions on Circuits and Systems*, 27(11):1102–1112, 1980.
- [42] C. D. Meyer. *Matrix Analysis and Applied Linear Algebra*. SIAM, 2001.
- [43] R. Lasseter and P. Piagi. Providing premium power through distributed resources. In *System Sciences, 2000. Proceedings of the 33rd Annual Hawaii International Conference on*, page 9 pp., January 2000.
- [44] N. Biggs. Algebraic potential theory on graphs. *Bulletin of the London Mathematical Society*, 29(6):641, 1997.
- [45] H. V. Henderson and S. R. Searle. On deriving the inverse of a sum of matrices. *SIAM Review*, 23(1):53–60, 1981.
- [46] R. A. Horn and C. R. Johnson. *Matrix Analysis*. Cambridge University Press, 1985.

## Appendix A. Proof of Theorem 3.7.

For simplicity and due to the same reasoning as in the proof of Theorem 3.6, we again augment the left-hand side of the load power balance (3.13) with frequency-dependent load  $D_0\dot{\theta}_0$  for some sufficiently small  $D_0 > 0$ . Consider the closed-loop system (3.12)–(3.14), with (3.14) formulated in the error coordinates  $\tilde{p}_i(t) \triangleq p_i(t) -$

$D_i \omega_{\text{avg}}$  for  $i \in \{1, \dots, n\}$ :

$$D_i \dot{\theta}_i = (P_i^* - D_i \omega_{\text{avg}} - a_{i0} \sin(\theta_i - \theta_0)) - \tilde{p}_i, \quad i \in \{1, \dots, n\}, \quad (\text{A.1})$$

$$D_0 \dot{\theta}_0 = P_0^* - \sum_{j=1}^n a_{j0} \sin(\theta_0 - \theta_j) \quad (\text{A.2})$$

$$k_i \dot{\tilde{p}}_i = P_i^* - \omega_{\text{avg}} D_i - \tilde{p}_i - a_{i0} \sin(\theta_i - \theta_0) - \sum_{j=1}^n L_{\text{comm},ij} \left( \frac{\tilde{p}_i}{D_i} - \frac{\tilde{p}_j}{D_j} \right), \quad i \in \{1, \dots, n\}. \quad (\text{A.3})$$

To establish our local stability result, we work on the Euclidean covering space  $\mathbb{R}^{n+1}$  of  $\mathbb{T}^{n+1}$ . In this flattened space, equilibria are repeated upon translation by  $2\pi$  in any canonical direction, and with a slight abuse of notation will also denote the by  $\theta$  the array of  $n+1$  of angles in the covering space. It will be convenient for us to explicitly remove the rotational invariance inherent in (A.1)–(A.3) by rewriting the dynamics in terms of the *difference coordinates*  $\delta \triangleq B^T \theta \in \mathbb{R}^n$ . Define the symmetric matrix  $M \triangleq B^T D^{-1} B \in \mathbb{R}^{n \times n}$ , and the *reduced quantities*  $\tilde{P}_r \triangleq (P_1^* - D_1 \omega_{\text{avg}}, \dots, P_n^* - D_n \omega_{\text{avg}})^T \in \mathbb{R}^n$  and  $D_r \triangleq \text{diag}(\{D_i\}_{i=1}^n) \in \mathbb{R}^{n \times n}$ . For notational compactness, we will also define  $A \triangleq \text{diag}(\{a_{i0}\}_{i=1}^n)$ . Since the topology of our problem is acyclic, it holds that  $\ker(B) = \emptyset$ , or equivalently that  $B \in \mathbb{R}^{(n+1) \times n}$  has column rank equal to  $n$  [44]. Consequently,  $M$  is a positive definite matrix. We collect a few results that are useful going forward in the following Lemma.

LEMMA A.1 (**Useful Identities**). *The following identities hold:*

- (i)  $AB^T L^\dagger \begin{bmatrix} P_0^* \\ \tilde{P}_r \end{bmatrix} = \tilde{P}_r$ ;
- (ii)  $B^T D^{-1} \begin{bmatrix} 0 \\ \tilde{p} \end{bmatrix} = D_r^{-1} \tilde{p}$ ;
- (iii)  $M = D_r^{-1} + \frac{1}{D_0} \mathbf{1}_n \mathbf{1}_n^T$ ;
- (iv)  $M^{-1} = D_r - \frac{1}{\sum_{i=0}^n D_i} D_r \mathbf{1}_n \mathbf{1}_n^T D_r$ .

*Proof.* To show (i), note first using (2.1) that

$$L = BAB^T = \begin{bmatrix} -\mathbf{1}_n^T \\ I_n \end{bmatrix} AB^T = \begin{bmatrix} -\mathbf{1}_n^T AB^T \\ AB^T \end{bmatrix},$$

and thus  $AB^T$  is obtained from the Laplacian matrix  $L$  by removing the first row. Since  $LL^\dagger = I_n - \frac{1}{n} \mathbf{1}_n \mathbf{1}_n^T$ , it holds similarly that  $AB^T L^\dagger$  is obtained by removing the first row of  $I_n - \frac{1}{n} \mathbf{1}_n \mathbf{1}_n^T$ . The result follows by noting that, by construction,  $P_0^* + \mathbf{1}_n^T \tilde{P}_r = 0$ . For (ii), we calculate directly that  $B^T D^{-1} [0, \tilde{p}^T]^T = B^T \text{blkdiag}(0, D_r^{-1} \tilde{p}) = D_r^{-1} \tilde{p}$ , as claimed. To show (iii), use (2.1) and calculate directly that  $M = B^T D^{-1} B = [-\mathbf{1}_n I_n] \text{blkdiag}(D_0^{-1}, D_r^{-1}) [-\mathbf{1}_n I_n]^T = \mathbf{1}_n \mathbf{1}_n^T / D_0 + D_r^{-1}$ . Item (iv) follows from (iii) by the Sherman-Morrison Formula for the inversion of sums of matrices [45].  $\square$

Using (i) and (ii) from Lemma A.1, the dynamics (A.1)–(A.3) can be equivalently rewritten as

$$\dot{\delta} = M(\tilde{P}_r - A \sin(\delta)) - D_r^{-1} \tilde{p}, \quad (\text{A.4})$$

$$k \dot{\tilde{p}} = \tilde{P}_r - A \sin(\delta) - (I_n + L_{\text{comm}} D_r^{-1}) \tilde{p}, \quad (\text{A.5})$$

where  $k = \text{diag}(\{k_i\}_{i=1}^n)$ . Now define the smooth potential functions  $H : \mathbb{R}^n \rightarrow \mathbb{R}$  and  $U : \mathbb{R}^n \rightarrow \mathbb{R}$  by  $H(\delta) \triangleq -\mathbf{1}_n^T A(\mathbf{1}_n - \mathbf{cos}(\delta))$  and  $U(\tilde{p}) \triangleq \frac{1}{2}\tilde{p}^T \tilde{p}$ . With this, the dynamics (A.4)–(A.5) can be further reformulated as

$$\frac{d}{dt} \begin{bmatrix} I_n & \mathbf{0} \\ \mathbf{0} & k \end{bmatrix} \begin{bmatrix} \delta \\ \tilde{p} \end{bmatrix} = \underbrace{\begin{bmatrix} M & D_r^{-1} \\ I_n & I_n + L_{\text{comm}} D_r^{-1} \end{bmatrix}}_Q \begin{bmatrix} \tilde{P}_r - \nabla_\delta H(\delta) \\ -\nabla_{\tilde{p}} U(\tilde{p}) \end{bmatrix}. \quad (\text{A.6})$$

We will first show that the asymmetric matrix  $Q$  is nonsingular, and in doing so conclude that the equilibria of (A.6) are given by  $\{(\delta, \tilde{p}) \in \mathbb{R}^n \times \mathbb{R}^n \mid \tilde{P}_r = \nabla_\delta H(\delta), \nabla_{\tilde{p}} U(\tilde{p}) = 0\}$ . To begin, consider the identity

$$Q = \begin{bmatrix} M & D_r^{-1} \\ I_n & I_n + L_{\text{comm}} D_r^{-1} \end{bmatrix} = \underbrace{\begin{bmatrix} M & I_n \\ I_n & D_r + L_{\text{comm}} \end{bmatrix}}_{=Q_1} \underbrace{\begin{bmatrix} I_n & \mathbf{0} \\ \mathbf{0} & D_r^{-1} \end{bmatrix}}_{=Q_2},$$

where  $Q_2$  is a positive definite diagonal matrix and  $Q_1$  is nonsingular. To verify the nonsingularity of  $Q_1$ , note that, by the *partitioned matrix inversion formula* [46, Sec. 0.7.3], nonsingularity of  $M$  implies that  $Q_1$  is nonsingular if and only if its Schur complement with respect to the  $M$  block, given by  $D_r + L_{\text{comm}} - M^{-1}$ , is nonsingular. Using Lemma A.1 (iv), we calculate that

$$D_r + L_{\text{comm}} - M^{-1} = L_{\text{comm}} + \frac{1}{\sum_{i=0}^n D_i} D_r \mathbf{1}_n \mathbf{1}_n^T D_r.$$

Thus, the Schur complement is the sum of the positive semidefinite matrix  $L_{\text{comm}}$  with one-dimensional zero eigenspace spanned by the vector  $\mathbf{1}_n$ , and the rank one matrix  $D_r \mathbf{1}_n \mathbf{1}_n^T D_r / \sum_{i=0}^n D_i$  with one-dimensional image spanned by  $D_r \mathbf{1}_n$ . Since  $\mathbf{1}_n^T (D_r \mathbf{1}_n) \neq 0$ , the kernel of  $L_{\text{comm}}$  is not perpendicular to the image of the second matrix, and the Schur complement is therefore positive definite. Hence  $Q$  is nonsingular, and the equilibria of (A.6) are given by the set  $\{(\delta, \tilde{p}) \in \mathbb{R}^n \times \mathbb{R}^n \mid \tilde{P}_r = \nabla_\delta H(\delta), \nabla_{\tilde{p}} U(\tilde{p}) = 0\} = \{(\delta, \tilde{p}) \in \mathbb{R}^n \times \mathbb{R}^n \mid \tilde{P}_r = A \mathbf{sin}(\delta), \tilde{p} = 0\}$ .

From Theorem 3.3, we have that the equations  $A \mathbf{sin}(B^T \theta) = \tilde{P}_r$  are solvable for a unique value  $\theta^* \in \bar{\Delta}_G(\gamma)$  (equivalently, the equations  $\tilde{P}_r = A \mathbf{sin}(\delta)$  are solvable for a unique value  $\delta^* \in [-\gamma, \gamma]^n$ ) if and only if the parametric condition (3.5) holds. Hence if (3.5) does not hold, the point  $(\delta^*, p^*)$  is not an equilibrium of closed-loop adaptive droop controlled system (3.12)–(3.14), and moreover no equilibria exist in the set  $[-\pi/2, \pi/2] \times \mathbb{R}^n$ . This establishes (ii)  $\Rightarrow$  (i), and we now continue with (i)  $\Rightarrow$  (ii).

To establish the local stability of  $(\delta^*, \tilde{p}^*)$ , we calculate the Jacobian matrix of (A.6) and evaluate it at the equilibrium point  $(\delta^*, \tilde{p}^*)$  to obtain

$$\begin{aligned} J(\delta^*, \tilde{p}^*) &= - \begin{bmatrix} I_n & \mathbf{0} \\ \mathbf{0} & k \end{bmatrix}^{-1} Q \begin{bmatrix} \nabla_\delta^2 H(\delta^*) & \mathbf{0} \\ \mathbf{0} & \nabla_{\tilde{p}}^2 U(\tilde{p}^*) \end{bmatrix} \\ &= - \begin{bmatrix} I_n & \mathbf{0} \\ \mathbf{0} & k^{-1} \end{bmatrix} Q_1 Q_2 \begin{bmatrix} \nabla_\delta^2 H(\delta^*) & \mathbf{0} \\ \mathbf{0} & I_n \end{bmatrix}. \end{aligned}$$

To examine the eigenvalues of the Jacobian, we proceed as follows. The eigenvalue problem  $J(\delta^*, \tilde{p}^*)v = \lambda v$  for  $\lambda \in \mathbb{C}$  and  $v \in \mathbb{R}^{2n}$  can be reformulated as a generalized

eigenvalue problem of the form

$$-Q_1 x = \lambda \left[ \begin{array}{c|c} I_n & \mathbf{0} \\ \hline \mathbf{0} & k \end{array} \right] \left[ \begin{array}{c|c} \nabla_{\delta}^2 H(\delta^*) & \mathbf{0} \\ \hline \mathbf{0} & I_n \end{array} \right]^{-1} Q_2^{-1} x, \quad (\text{A.7})$$

where

$$x = Q_2 \left[ \begin{array}{c|c} \nabla_{\delta}^2 H(\delta^*) & \mathbf{0} \\ \hline \mathbf{0} & I_n \end{array} \right] v \in \mathbb{R}^{2n}.$$

In particular, note that  $-Q_1$  is negative definite, and the matrix multiplying  $\lambda x$  on the right side of (A.7) is diagonal. Moreover, it is easy to see that the matrix  $\nabla_{\delta}^2 H(\delta^*) = \text{diag}(\{a_{i0} \cos(\delta_i^*)\}_{i=1}^n)$  is positive definite if and only if the droop control stability condition (3.5) holds, since only in this case we have that  $\delta^* \in [-\gamma, \gamma]^n$  for some  $\gamma < \pi/2$ . As in the proof of Theorem 3.3, we can appeal to the *Courant-Fischer Theorem* [42] to conclude that eigenvalues of the Jacobian are real, and in particular, lie strictly in the left half plane. This completes the proof of Theorem 3.7.